

Computational and Experimental Study on the Discharge Model of a 20 Amperes Emission Current Hollow Cathode

Mingming Sun^{1,*} , Chao Liu¹ , Zengjie Gu¹ 

¹China Academy of Space Technology – Lanzhou Institute of Physics – Science and Technology on Vacuum Technology and Physics Laboratory – Lanzhou/Gansu – China.

*Correspondence author: smmhappy@163.com

ABSTRACT

The discharge characteristics of hollow cathode directly affect the performance of thruster. In order to obtain the plasma parameters of the 20 A emission current hollow cathode, COMSOL software is used to simulate the potential distribution, neutral fluid distribution and plasma parameters of the cathode, then the test is carried out to verify the simulations. The results show that the fluid velocity in the emitter region is about 20 ms^{-1} and is uniform in the radial direction. The electron density throughout the cathode discharge zone is almost uniform within the range of $1.09 \times 10^{20} \sim 1.2 \times 10^{20} \text{ m}^{-3}$. The electron temperature increased from 2.8 to 4.9 eV throughout the cathode discharge zone. The electron collision frequency is in the order of 10^{23} Hz . The test results show that the electron temperature is increased from 2.4 to 5.2 eV from outlet of the emitter region to the plume region, and which presents an opposite trend to the electron density. There is a small error between the test results and the simulation results, and this error is mainly caused by the flow boundary setting.

Keywords: Cathode discharge; Numerical simulation; Discharge parameters; Plasma diagnosis.

INTRODUCTION

A 30-cm diameter ion thruster is a high power (two work modes, 3 and 5 kW), high thrust (100 mN in 3 kW and 200 mN in 5 kW) ion thruster, which is designed for the new generation large-scale truss-type satellite platform in China (Sun *et al.* 2020). In order to meet the performance demands of a 30-cm diameter ion thruster, a hollow cathode with a nominal 20 A emission current has been designed and manufactured as the primary electron source (Sun *et al.* 2018a). The hollow cathode is a conventional heated orifice type and uses LaB₆ material as the emitter. The heating coils around the heater (which is made of rhenium-tungsten) makes the emitter reaching its work function through ohmic heating (Goebel *et al.* 2005). Meanwhile, the thermal electrons collide with neutrals and produce a high-density plasma. The plasma density of thruster and extracted ion beam are all depended on the electron temperature and emission current of the hollow cathode in the discharge chamber (Mikellides *et al.* 2006a). Therefore, there is a great significance to simulate and analyze the discharge process of hollow cathode to improve the performance of ion thruster.

Received: Jul. 29, 2021 | Accepted: Oct. 18, 2021

Peer Review History: Single Blind Peer Review.

Section editor: Rodrigo Palharini



This is an open access article distributed under the terms of the Creative Commons license.

As shown in Fig. 1a, the hollow cathode discharge zone can be divided into three regions, which are emitter region, orifice region and plume region, respectively. The whole discharge process can be regarded as the process of high-density thermal electrons, that generated in emitter region and through the orifice region, then accelerated towards plume region by axial electric field.

Katz *et al.* (2002) assumed the electron in the cathode discharge zone as a fluid and the neutral gas density in the emitter region and orifice region as a homogeneous distribution, then established a one-dimensional fluid simulation model for the NSTAR ion thruster Ba-W hollow cathode (which emission current is 3.26 A, and xenon gas flow rate is 3.7 SCCM). Based on the model, the characteristic parameters of the plasma in the emitter and orifice region are calculated. The simulations show that the cathode orifice region plasma density peak appears in the center line of the orifice, while the plasma density on both ends of the orifice region are relatively low. The electron temperature in the whole orifice region is in the range of 1.1 ~ 1.5 eV, and increases to about 2 ~ 3 eV after entering the discharge chamber of the thruster.

Katz *et al.* (2002) calculate that about 1/3 of the total number of electrons emitted from the Ba-W cathode are generated in the orifice region, and electron temperature simulation results are in good agreement with the test results of Malik *et al.* (2000). In addition, Katz *et al.* (2002) predicted the orifice erosion by calculated ion current density, and the predicted results are compared with the 8200-h life test of the Ba-W cathode carried out by Polk *et al.* (2005). The results show that the cathode erosion trend is consistent with the experimental results. Mikellides *et al.* (2005) established a discharge model for the hollow cathode of nuclear electric xenon ion thruster system (NEXIS) ion thruster (with the emission current of 25 A). After the work parameters are substituted into the model, the calculated results show that the plasma density in the emitter region is in the range of $10^{19} \sim 10^{20} \text{ m}^{-3}$, and the electron current density and electron temperature are in the range of $1 \times 10^4 \sim 10^5 \text{ A}\cdot\text{m}^{-2}$ and 1 ~ 2 eV, respectively. Plasma potential in the emitter region is in the range of 5 ~ 14 V, which is obviously lower than that in the orifice region (which is in the range of 15 ~ 30 V), and energy of the ions bombarding to the surface of the emitter is only about 20 eV for the reason of low plasma potential and the high collision frequency and scattering rate of neutrals on the emitter surface.

Jameson *et al.* (2005) build a zero-dimensional discharge model of TH15 hollow cathode (the emission current is 13 A) for NSTAR ion thruster to obtain the plasma discharge characteristics. The simulations have shown that the pressure of neutral gas expresses a significant decreasing trend from emitter region to orifice region. The electron temperature increased continuously in the whole cathode discharge zone, and the average electron temperature in the orifice region is 2.3 eV and the variation is no more than 1 eV. The calculated results are consistent with the test results, and the results prove that the zero-dimensional discharge model is very accurate. Goebel *et al.* (2005) measured potential and density profiles in the NEXIS hollow cathode discharge, which indicated that the magnitudes of plasma density are 10^{21} and 10^{23} m^{-3} in the emitter and orifice region, respectively, and the electron temperature within the cathode is found to be only 1 to 2 eV. After the electrons extracted to the plume region, the electron density decreases rapidly to $1 \times 10^{18} \text{ m}^{-3}$ along with the increasing distance from the exit of cathode orifice.

Gabriel (2017) investigated the discharge process of hollow cathode used with Argon gas by COMSOL in 2017, and two different simulations (heaterless cathode and orificed cathode) were performed. The simulation results of the orifice hollow cathode with anode and flow showed that the peak plasma density (about $5 \times 10^{20} \text{ m}^{-3}$) occurs at the entrance to the orifice, and the peak electron temperature (6 eV) occurs at 5 mm downstream from the cathode inlet. In the course of the simulation, it is difficult to achieve convergence unless the laminar flow interface is used and coupled through the absolute pressure and flow velocity. In addition, Gabriel (2017) indicates that COMSOL could become a useful tool in carrying out quick and inexpensive parametric studies of the effects of geometry after convergence issues solved.

These previous studies mentioned above have well indicated that the whole discharge process of hollow cathode can be simulated by establishing a cathode discharge model, and more accurate plasma parameters can be obtained. By using COMSOL multiphysical field coupling software (COMSOL 2016), this paper establishes a discharge model and studies the plasma characteristics throughout the discharge zone of a 20 A emission current hollow cathode for 30-cm diameter ion thruster. In the next section, model geometry, parameters setting, and simplification of discharge process simulation is introduced in detail, and some boundary conditions are given by experimental data and adjusted (within the reasonable error range of the test results) to achieve the convergence. In addition, plasma parameters measurement by using Langmuir probe is carried out to verify the simulations, and comparison results are used to verify the accuracy of the hollow cathode discharge model.

STRUCTURE AND WORK PARAMETERS OF THE CATHODE

Fig. 1a shows the structure of the 20 A emission current hollow cathode. The emitter is a cylindrical structure of LaB_6 material with a length of 10 mm and an inner diameter of 4 mm. Orifice plate is an inverted conical structure of tungsten material with a thickness of 2.5 mm, and the diameter of the cathode orifice is 2 mm. The keeper is a tantalum round plate with a central aperture, and the thickness and the diameter of the aperture is 1 and 5 mm, respectively. The cathode tube is made of tantalum material with an inner diameter of 8 mm, and the length is 50 mm. Neutral xenon gas is injected into the inlet of the cathode tube through a gas insulator (a ceramic component connected to the inlet of the cathode to isolate the gas discharge process towards the supply tube). A graphite shield with apertures makes the velocity of the xenon flow more uniform, in addition, it can also adsorb active gases, such as water vapor, oxygen and so on. As shown in Fig. 1a, an electron absorption wall in the plume region is set 5 mm away from the outlet of the keeper to simulate the anode plate, and the upper and lower walls of the area between the keeper and the anode is set as electron cross boundary. Emitter region, where the emitter temperature is heated to over 1500 °C, is the one of the main discharge zones, thermal electrons emit from the surface of the emitter and create thermal electron currents (Sun *et al.* 2018b). After heating for about 400 s, a voltage is applied between the keeper and emitter to generate an electric field in the cathode discharge zone to extract and accelerate the electrons, which will then collide with the neutral xenon atom in emitter region, then the heating of the emitter is terminated. Xenon ions and secondary electrons are generated by the collision ionization when the electron is accelerated to 12.13 eV (the first order ionization energy of xenon atoms). In this process, a part of electrons is accelerated by electric field continuously and involves in collisions; the other part is extracted from the orifice of the keeper, forms the emission current and injects into the discharge chamber of ion thruster as primary electrons (primary electron energy is lower, about 2 ~ 3 eV) (Wirz and Katz 2005). Ions bombard the surface of the emitter under the effect of electric field and are neutralized by the electrons and maintain the temperature of the emitter, so that the emitter could maintain the thermal electron emission process. Fig. 1b shows the mesh model of the cathode, and the mesh setting choose the controlled mesh. Element size adopts dynamics calibration, and which is set to normal. Considering that the inner diameter of the emitter is 4 mm, the minimum element size is set to 0.04 mm, which is 1/100 of the inner diameter, and the maximum element size is set to 0.5 mm, which is 1/100 of the length of the cathode tube. The purpose of setting is to reduce the calculation time while ensuring the accuracy of the simulation results.

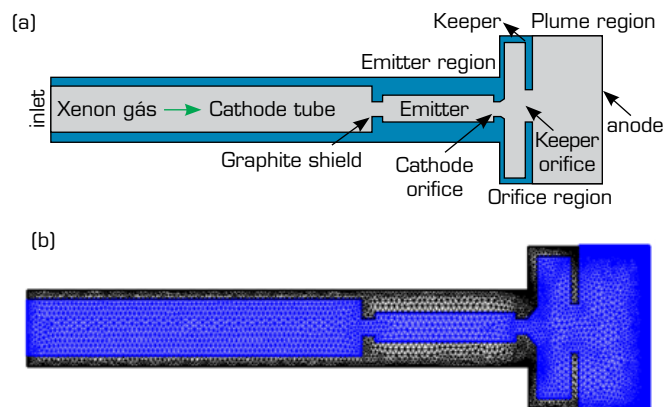


Figure 1. The structure and the mesh model of the hollow cathode.
(a) The structure of hollow cathode structure; (b) Mesh model.

Table 1 gives the parameters of 20 A emission current cathode. LaB_6 was adopted as the emitter material because it can tolerate worse environment and avoid emitter poisoning, although its high work function needs a higher temperature to generate thermal electrons. The start-up time is defined as from the start of cathode heater working until the cathode emits the rated emission current, and it generally is within 7 min. Pulsed power provides 800 ~ 1100 V/10 s impulse voltage on the keeper, and then the cathode emission current reached its rated value and the cathode reaches self-heating discharge state, pulsed power is turned off. A constant voltage is provided on the keeper, and the potential difference between the keeper and the emitter formed an axial electric field to draw the thermal electrons from the emitter region to the plume region.

Table 1. Work parameters of 20 A emission current cathode.

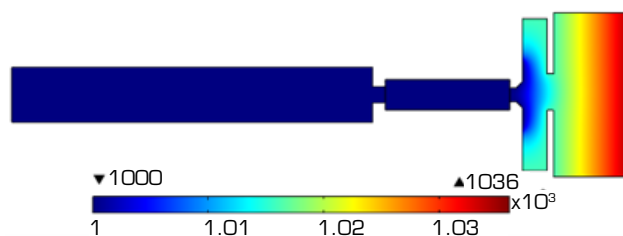
Mass flow (SCCM)	Keeper voltage (V)	Anode voltage (V)	Heat current (A)	Emitter material	Start-up time (s)	Ignition pulse
1.8	1010	1036	7.5	LaB ₆	< 420	800 ~ 1100 V/10 s

The parameters of 20 A emission current cathode are used to set the boundary conditions of the cathode discharge model to solve the potential distribution, the fluid simulation within the cathode tube, the neutral atom density distribution and so on.

DISCHARGE MODEL AND SIMULATION RESULTS

The discharge process of the hollow cathode is simulated by COMSOL software, and the electrostatics (ES) module, laminar flow (SPF) module, drift diffusion (DD) module are coupled to simulate the discharge process. Electrostatics and SPF modules are used to obtain the parameters such as the voltage potential, fluid velocity, pressure and so on. The whole process of the simulation is divided into steady state solution (step 1) and transient solution (step 2). Due to the electric field distribution and pressure distribution within, the cathode does not have a large change in the process of discharge. However, the plasma density changing with time is significant. The model is set to perform steady-state solution first, that is, calculate the electric field distribution and pressure distribution inside the cathode, and the calculation results are stored in the step 1. Then, the transient solution is performed. Meanwhile, the results stored in the step 1 are used to calculate the neutral density, collision reaction coefficient, collision energy loss and other parameters, and the electron temperature, plasma density and others are further calculated in step 2.

As described above, firstly, the electric potential distribution in the discharge area of the cathode should be solved. According to the thruster power supply relationship, the voltages of the keeper and the anode are float on the screen voltage. As shown in Fig. 2, the keeper is applied at 1016 V, and the inner surface of the emitter, cathode tube and the outer surface of the cathode orifice are applied at a voltage of 1000 V. It is because in the process of cathode discharge, these regions can be considered to have the same potential as the screen grid (which is the lowest potential of the ion thruster with the value of 1000 V). The boundary of the plume region is set as 1036 V to simulate the anode voltage. For static magnetic fields ($\partial B/\partial t=0$), the electric field can be expressed as the gradient of the electric potential, $E=-\nabla V$, the negative sign comes from the convention that the electric field always points in the direction of ion motion. In addition, the electric field simulation is based on the assumption that plasma is quasi-steady and the self-consistent electric field of plasma is ignored.

**Figure 2.** Electric potential distribution of the hollow cathode.

Secondly, the pressure and the neutral density in the discharge zone of the cathode should be investigated. According to the previous test results of the same type cathode (Sun *et al.* 2015), before the discharge begins, the velocity of neutral gas at the outlet of the orifice is in a low level, and below 0.3 Ma. As shown in Fig. 3, the fluid in the discharge zone is considered as incompressible and turbulence is ignored. The temperature of the fluid is set as 300 K to obtain the fluid parameters before gas discharge (Sun *et al.* 2018b). All the inner walls of the discharge zone are set as the no-slip boundary, which means the fluid velocity on the wall is zero. According to the previous measurement results and calculations by Fluent software (Sun *et al.* 2015), the boundary of the inlet

and the outlet are set as a pressure condition with the values 50 and 0.05 Pa, respectively, and the flow direction is perpendicular to the inlet section. The initial pressure of the discharge zone is set as 0.01 Pa, and the pressure distribution and the fluid velocity are shown in Fig. 3a and 3b by assuming the gas to be a steady flow. The simulations in ES module and SPF module are steady simulation. The simulation in DD module is a transient simulation, and the time range is set from 10^{-8} to 10^{-1} s to ensure the plasma properties are evolving with time until steady state conditions are reached.

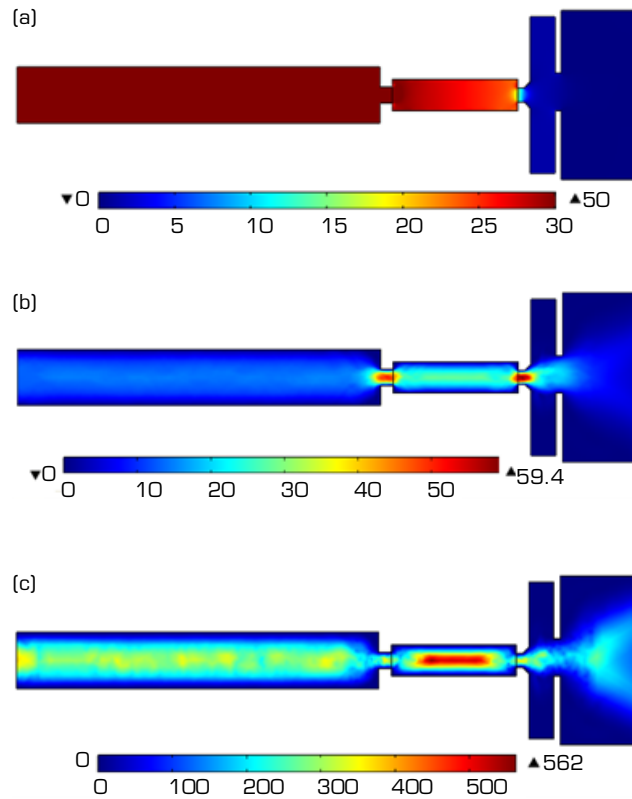


Figure 3. Pressure, fluid velocity and Reynolds number in the discharge region of the cathode. (a) Pressure distribution (Pa); (b) Fluid velocity (ms^{-1}); (c) Reynolds number.

According to the results shown in Fig. 3, the pressure does not present a significant gradient in the cathode tube for the blocking effect of the graphite shield, and the pressure value is in the range of 45 ~ 50 Pa. However, in the emitter region, the pressure shows a significant gradient, and which decreases along the direction of the graphite shield to the cathode orifice due to the throttling effect of the orifice. Figure 3b shows that the fluid velocity suddenly increased from inlet to outlet in the orifice due to the Laval effect (Dong *et al.* 2015), and the fluid velocity in the middle region is about 20 ms^{-1} and is uniform distribution radially. Figure 3c gives the Reynolds number obtained by COMSOL, which is related to the stability of the numerical discretization. The results show that the Reynolds number throughout the discharge zone is in the range of 220 ~ 562. Therefore, the fluid flow status is treated as laminar flow for the calculated Reynolds number is less than 1200. Boundary conditions are set as nonslipping.

The drift diffusion module is mainly used to calculate the electron temperature, electron density for the further discharge process simulation in the chamber of the ion thruster. Cathode sheath is determined by the heat loss and work function of the emitter, electron temperature and plasma resistance. In addition, the intense collision and continuous ionization process in the emitter region will lead to the decrease of cathode sheath potential on the surface of the emitter. According to the previous calculation results (Sun *et al.* 2018b), cathode sheath is treated as a fixed value on the emitter surface to simplify the simulation, and the value is in the range of 8 ~ 10V (at an emitter heat loss of 10.26 W). The drift diffusion module which includes the electron continuity equation, electron flux equation and energy equation. The electron continuity equation is shown as Eq. 1,

$$\frac{\partial n_e}{\partial t} + \nabla \Gamma_e = R_e - (u \cdot \nabla) n_e \quad (1)$$

where n_e is electron density, Γ_e is the electron flux in the cathode discharge zone, μ is the electron velocity, R_e is the electron generation rate and the unit is $\text{m}^{-3} \cdot \text{s}^{-1}$. The electrons are generated from elastic collision, excitation collision and ionization collision, and the expression of reaction rate coefficient for xenon in different collision type had been given by Miller *et al.* (2002). The different reaction rate coefficients are denoted by k_1 , k_2 and k_3 , respectively. Meanwhile, all the different reaction rate coefficients have the similar expressed equation as $\langle \sigma v \rangle$ (where σ is collision cross section, and v is the frequency of collisions between particles and determined by the electron temperature T_e) (Book 1987). The elastic collision is ignored for which produce almost no Maxwellian electron, and, in most cases, the energy transfer is predominant. Then, the electronic excitation reaction rate r_2 and ionization reaction rate r_3 can be expressed as $k_2 n_0 n_e$ and $k_3 n_0 n_e$. Therefore, R_e is expressed as Eq.2.

$$R_e = r_2 + r_3 = k_2 n_0 n_e + k_3 n_0 n_e \quad (2)$$

The electron flux Γ_e can be given by drift diffusion equation, which is shown as Eq.3,

$$\Gamma_e = -(\mu_e \cdot E) n_e - D_e \cdot \nabla n_e \quad (3)$$

where E is the self-consistent electric field (expressed as $E = -\nabla V$), μ_e is electron migration coefficient, which is given by $\mu_e = e/mv(1 + \Omega_e^2)$. The collision frequency ν_{en} between electrons and neutral atoms, and ν_{ei} between electrons and ions are considered in the cathode discharge model. Meanwhile, the collision process between ions and ions, ions and atoms are ignored for the reason that the electrons coming from these collisions are negligible relative to the electrons generated by electron-atom collisions. ν_{en} and ν_{ei} are given by Katz *et al.* (2004) and Book (1987), respectively. The term of electron Hall parameter correction Ω_e is ignored as there is no magnetic field in the cathode discharge zone (Goebel and Katz 2008). D_e is the electron diffusion coefficient which has Einstein's relation with μ_e , and expressed as $D_e = \mu_e T_e$. The energy balance equation is shown in Eq.4,

$$\frac{\partial n_\varepsilon}{\partial t} + \nabla \Gamma_\varepsilon + \mathbf{E} \cdot \Gamma_e = S_{en} - (u \cdot \nabla) n_\varepsilon \quad (4)$$

where n_ε is the electron energy density and Γ_ε is the electron energy density flux, which all have relations with μ_e , n_e and T_e . S_{en} is the energy loss of electron collision, which consists of three parts, elastic collision energy loss d_{e1} , first order and second order ionization energy loss of xenon atoms, and denoted by d_{e2} and d_{e3} . The parameters setting of the drift diffusion module in COMSOL are shown in Table 2, where k and m_e are Boltzmann constant and electron mass, respectively.

The key parameters shown in Table 2 are substituted into the cathode discharge model, and according to the electric potential distribution, gas pressure and fluid velocity, etc. obtained in Fig. 2 and Fig. 3, the electron density, electron temperature, neutral density and electron collision frequency could be calculated, as shown in Fig. 4a-d.

Figure 4a shows that the electron density throughout the cathode discharge zone is relatively uniform and within the range of $1.09 \times 10^{20} \sim 1.2 \times 10^{20} \text{ m}^{-3}$. Compared with the previous results (Goebel *et al.* 2005; Katz *et al.* 2004; Mikellides *et al.* 2005), the electron density is basically consistent with the previous calculations (especially the NEXIS cathode at 25 A and 5.5 SCCM). The electron density in the emitter region is highest due to the highest neutral density in this area (electron density is proportional to the neutral density in quasi-steady ionization), and the electron density in the orifice region is lower than that in the emitter region, but the electron density in both regions is in the same order of magnitude. The reason is that the neutral density is lower than that in emitter region, correspondingly, a lower electron density. In addition, the boundary condition of the orifice wall is set as the electron absorption boundary, and a part of the electrons which enter the orifice region are deposited on the orifice wall. On the contrary, the boundary condition of the emitter wall is set as the electron reflection boundary, and which means the number of electrons will not be reduced.

Table 2. Parameters setting of the drift diffusion module.

Parameters	Expression	Description
k_1	$1.99 \cdot 10^{-14} T_e^{0.93} e^{0.41/T_e}$	Elastic rate coefficient
k_2	$1.93 \cdot 10^{-19} e^{11.6/T_e} [T_e^{0.5} (8eT_e/\pi/m_e)^{0.5}]$	Excitation rate coefficient
k_3	$10^{-20} (3.97 + 0.643 T_e - 0.0368 T_e^2) \times e^{12.127/T_e} (8eT_e/\pi/m_e)^{0.5}$	Ionization rate coefficient
r_1	$k_1 n_0 n_e$	Elastic collision reaction rate
r_2	$k_2 n_0 n_e$	Electronic excitation reaction rate
r_3	$k_3 n_0 n_e$	Ionization reaction rate
$d_{e1}; d_{e2}; d_{e3}$	0; 8.31; 12.13	Energy loss of elastic collision, excitation and ionization
R_e	$r_2 + r_3$	Electron production rate
S_{en}	$-e(r_1 d_{e1} + r_2 d_{e2} + r_3 d_{e3})$	Collision power loss
σ_{en}	$6.6 \cdot 10^{-19} [T_e/4 - 0.1]/[1 + (T_e/4)^{1.6}]$	Collision cross section
$\ln \Lambda$	$23^{0.5} \log(10^6 n_e / T_e^3)$	Coulomb logarithm
ν_{en}	$\sigma_{en} n_0 (8kT_e/\pi/m_e)^{0.5}$	Electron-neutral collision frequency
ν_{ei}	$2.9 \cdot 10^{-12} n_e \ln \Lambda / T_e^{1.5}$	Electron-ion collision frequency
μ_e	$e/[m_e (\nu_{en} + \nu_{ei})]$	Electron migration coefficient

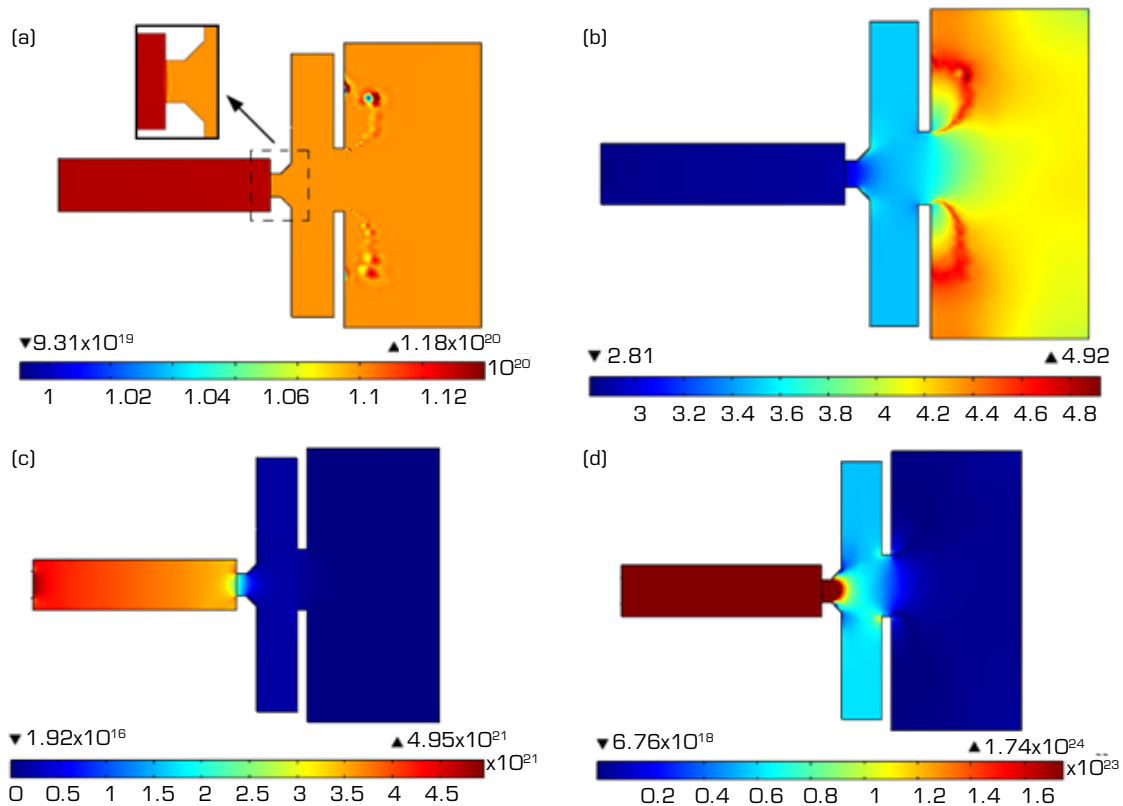

Figure 4. The discharge parameters in the discharge region of the cathode. (a) Electron density (m^{-3}); (b) Electron temperature (eV); (c) Neutral density (m^{-3}); (d) Electron collision frequency (Hz).

Figure 4b expresses the electron temperature distribution in the discharge zone of the cathode. The electron temperature in the orifice region is higher than that in the emitter region, while the electron temperature in the plume region is the highest and express a distinct spurting shape. This is mainly due to the electric potential distribution, where the electric potential is increased from the keeper to the anode plate, and the electric field line from the orifice to the anode is curved (shown in Fig. 2). In addition, Fig. 4b indicates that the electron temperature throughout the cathode discharge zone is continuously increasing, which increased from 2.8 to 4.9 eV over the distance from the emitter region to the plume region. The variation of electron temperature shown in Fig. 4b has a similar trend with the previous researches (Goebel *et al.* 2005; Katz *et al.* 2002; Katz *et al.* 2004).

Figure 4c mapped a neutral density distribution in the cathode discharge zone, which in the emitter region is in the order of 10^{21} m^{-3} . The neutral density distribution depends on the pressure distribution shown in Fig. 3a, and which is decreasing throughout the cathode discharge zone for the gas pressure attenuation. The results shown in Fig. 4d clearly show that there is intense electron-neutral collision process in the emitter and in the orifice regions. Therefore, electron collision frequency is the highest in these regions for the high neutral density and electron density and the frequency is in the order of 10^{23} Hz . By contrast, although there are collisions in the plume region, the electron collision frequency is much lower than that in the internal discharge zone of the cathode due to the relatively sparse particle density.

TEST RESULTS AND COMPARISON

In order to verify the accuracy of 20 A emission current cathode discharge model, a discharge performance test on TS-5B facility of Lanzhou Institute of Physics (LIP) was carried out. Diameter and length of the facility are 800 and 1000 mm, respectively, and the vacuum system can maintain a vacuum degree of $1 \times 10^{-3} \text{ Pa}$ with a pumping speed of $1000 \text{ L}\cdot\text{s}^{-1}$ during the test. The diagnostic instruments include Langmuir probe, thermal imager, temperature sensors etc. As shown in Fig. 5a, the cathode is mounted on a support, and a probe is aligned with the center line of the cathode orifice. In addition, an anode plate is fixed 5 mm far from the outlet of the keeper. For test process, a xenon gas with mass flow rate of 1.8 SCCM, and after the cathode is heated for 240 s with 7.5 A heating current, the temperature of the emitter is measured by an infrared thermometer as about $1450 \text{ }^\circ\text{C}$ (Sun *et al.* 2017). Meanwhile, a high voltage ignition pulse is applied on the keeper. After the keeper and the anode enter the constant current mode, the heating power is turned off. The self-heating discharge state of the cathode is successfully established and electrons are continuously emitted, and, at this time, the temperature of the emitter is stable at 1500 to $1600 \text{ }^\circ\text{C}$.

A Langmuir probe with the diameter of 0.2 mm is used for the plasma parameters measurement. The probe started from the plume region (closed to the anode plate) and is driven by a stepping motor to slowly pass through the orifice region, and finally stops near the emitter outlet, and the whole measuring range is 9 mm. The influence of the probe inserted into the discharge zone on the plasma properties is ignored for the reason that the effect of the test instrument on the plasma is not clear and there is no means of evaluation present. The measurement error of the electron temperature is about in the range of 5 ~ 15% (Mikellides *et al.* 2006b); however, that of the electron density is not clear. Figure 5a is the working picture of the cathode in the self-heating discharge state, and Fig. 5b shows the test position of Langmuir probe, and the electron density in different position of the cathode discharge zone is obtained. The test results show that the electron temperature from outlet of the emitter region to plume region increased from 2.4 to 5.2 eV. The electron density is generally on the order of $10^{20}\cdot\text{m}^{-3}$ from outlet of the emitter region to the outlet of the keeper orifice, and the closer to the anode, the lower the electron density is.

The comparison of the test results and the simulation results are shown in Fig. 6a and b. Figure 6a indicates that the electron temperature from outlet of the emitter region to plume region is increasing continuously for the acceleration effect by the electric potential. The test results of electron temperature are lower than the simulations in the orifice region, a probable reason of this fact is that the boundary setting of cathode inlet in SPF module adopts a pressure condition with the value of 50 Pa (Sun *et al.* 2015). However, this value is based on the flow rate, the measured pressure at the inlet of the gas supply tube, the calculations of

flow conductivity of the supply tube, and then obtained through simulation by Fluent. In addition, due to the influence of the gas insulator on gas flow is ignored, as well as measurement and calculation errors. Therefore, the actual cathode inlet pressure is higher than the 50 Pa pressure setting, and the test results of the neutral density in the discharge zone is actually higher than the simulations, which can be verified according to the electron density given in Fig. 6b. When the cathode is into the self-heating discharge state, the plasma in all discharge areas inside the cathode is in thermal equilibrium, the neutral density, electron density and ion density are approximately equal. As shown in Fig. 6b, the test results of electron density are higher than simulations, so the neutral density is also higher than the simulations (in quasi-steady ionization).

According to Goebel and Katz (2008), it can be concluded that if the neutral density is lower, then for the plasma ambipolar diffusion process in the discharge zone under self-sustained state, the mobility of electrons is much greater than that of ions, and the neutral density is inversely proportional to the ambipolar diffusion coefficient. Therefore, the ambipolar diffusion coefficient is greater under this condition. In addition, the diffusion coefficient is higher in lower neutral density case, which means the lower the chance of collisions between charged particles, and the electron temperature is higher for the less energy loss, that is, there is an inverse relationship between the electron temperature and the plasma density. Therefore, Fig. 6b expresses an opposite result compared to Fig. 6a in the range of 1 to 4 mm away from the outlet of the emitter region. According to previous results (Katz *et al.* 2004), especially the test results of NEXIS cathode at 25 A emission current and 5.5 SCCM (similar emission current and gas flow), which show that plasma density decreased from 10^{20} to 10^{19} m^{-3} and electron temperature increased from 3 to 5 eV in the distance of 0.01 m from orifice entrance. The variation trend of electron density and electron temperature obtained from the test is consistent with the previous results of NEXIS cathode.

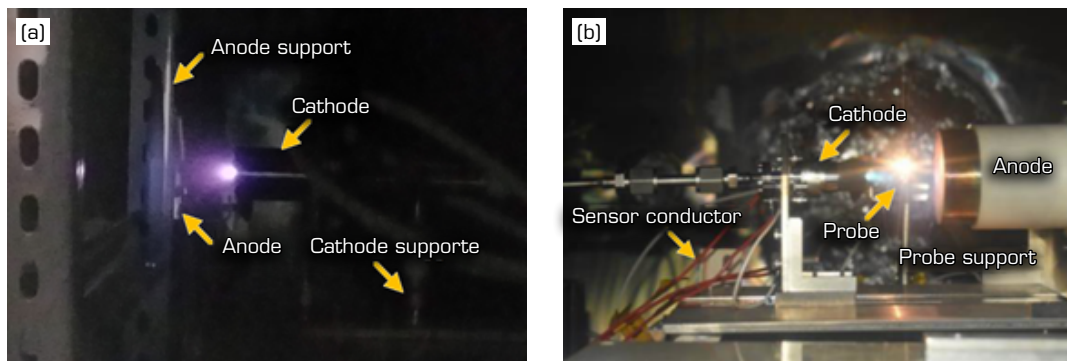


Figure 5. Discharge test of the hollow cathode. (a) The test apparatus; (b) Test position of Langmuir probe.

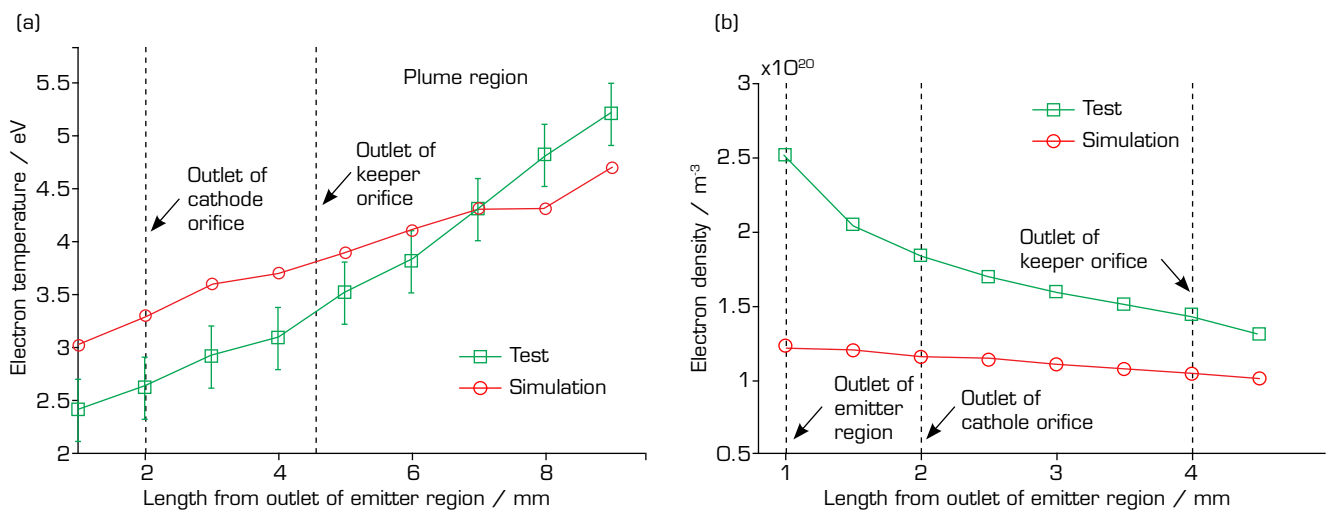


Figure 6. The comparison of the test and the simulation results. (a) Electron temperature (eV); (b) Electron density (m^{-3}).

CONCLUSIONS

This paper establishes a discharge model and obtains discharge plasma parameters of the 20 A emission current hollow cathode, and then a discharge performance measurement test is carried out to verify the simulations. The simulation results show that the calculations can achieve a better convergence with the assumption of the gas to be a steady flow, and the fluid inside the discharge zone is set as incompressible flow, and the pressure boundary conditions at the inlet and outlet are adopted. Neutral fluid velocity in the emitter region is about 20 ms^{-1} and is uniform distribution radially, and the pressure decreased along the direction of the graphite shield to the cathode orifice due to the throttling effect of the orifice. The electron density throughout the cathode discharge zone is within the range of $1.09 \times 10^{20} \sim 1.2 \times 10^{20} \text{ m}^{-3}$. Due to the electric potential distribution, the electron temperature in the plume region is the highest and expresses a distinct spurting shape, and the electron temperature increased from 2.8 to 4.9 eV over the distance from the emitter region to the plume region. The electron-neutral collision is the order of 10^{23} Hz , and which is most intense in the emitter region and the orifice region. The electron collision frequency in the plume region is much lower than that in the internal discharge zone due to the relatively low particle density. The comparison errors between test results and simulations are small, and errors are mainly caused by the flow boundary setting of the cathode model. Due to an inverse relationship between the electron temperature and the plasma density, the variation trend of the electron density expresses an opposite result compared to that of the electron temperature in the range of 1 to 4 mm away from the outlet of the emitter region. The neutral density distribution in the discharge zone has a significant influence on the simulation results of plasma parameters. If the flow boundary conditions can be accurately obtained, then the more accurate distribution of neutral density can be obtained. In this case, COMSOL can be a useful tool for studies of cathode discharge parameters. The study result of this paper is used to determine the discharge parameters of the 20 A emission current hollow cathode and in the 30-cm diameter thruster that will be used.

AUTHORS' CONTRIBUTION

Conceptualization: Sun M; **Methodology:** Sun M; **Investigation:** Sun M and Liu C; **Writing – Original Draft:** Sun M; **Writing – Review and Editing:** Sun M and Gu Z; **Funding Acquisition:** Sun M; **Resources:** Liu C; **Supervision:** Sun M.

DATA AVAILABILITY STATEMENT

All data sets were generated or analyzed in the current study

FUNDING

National Natural Science Foundation of China,
[<https://doi.org/10.13039/501100001809>]
Grant No. 61901202.

ACKNOWLEDGEMENTS

Not applicable.

REFERENCES

- Book DL (1987) *NRL Plasma Formulary*. Washington: Naval Research Laboratory.
- COMSOL (2016) COMSOL® software version 5.2a. Burlington: COMSOL Inc. [accessed Mar. 11 2017]. <http://cn.comsol.com/product-update/5.2a-cluster-computing>
- Dong XM, Li J, Chen JJ (2015) [The numerical simulation of natural gas distribution in heaterless cathode]. *Vacuum and Cryogenics* 5:283-286. Chinese. <https://doi.org/10.3969/j.issn.1006-7086.2015.05.008>
- Gabriel SB (2017) COMSOL modelling of hollow cathodes. Paper presented 35th International Electric Propulsion Conference. Atlanta, Georgia, United States of America. [accessed Jan 12 2020]. http://electricrocket.org/IEPC/IEPC_2017_487.pdf
- Goebel DM, Katz I (2008) *Fundamentals of electric propulsion: Ion and hall thrusters*. New York: John Wiley & Sons.
- Goebel DM, Jameson KK, Watkins RM, Katz I, Mikellides IG (2005) Hollow cathode theory and modeling. *J Appl Phys* 98:113302. <https://doi.org/10.1063/1.2135417>
- Jameson KK, Goebel DM, Watkins RM (2005) Hollow cathode and keeper-region plasma measurements. Paper presented 41st AIAA/ASME/SAE/ASEE Joint Propulsion Conference & Exhibit. AIAA; Tucson, Arizona, United States of America. <https://doi.org/10.2514/6.2005-3667>
- Katz I, Anderson J, Polk J, Brophy JR (2002) A model of hollow cathode plasma chemistry. Paper presented 38th AIAA/ASME/SAE/ASEE Joint Propulsion Conference and Exhibit. AIAA; Indianapolis, Indiana, United States of America. [accessed Jul 23 2020]. <https://trs.jpl.nasa.gov/bitstream/handle/2014/9392/02-1601.pdf>
- Katz I, Mikellides IG, Goebel DM (2004) Model of the plasma potential distribution in the plume of a hollow cathode. Paper presented 40th AIAA/ASME/SAE/ASEE Joint Propulsion Conference and Exhibit. AIAA; Lauderdale, Florida, United States. <https://doi.org/10.2514/6.2004-4108>
- Malik AK, Montarde P, Haines MG (2000) Spectroscopic measurements of xenon plasma in a hollow cathode. *J Phys D: Appl Phys* 33:2307. <https://doi.org/10.1088/0022-3727/33/16/316>
- Mikellides IG, Katz I, Goebel DM, Polk J (2005) Theoretical modeling of a hollow cathode plasma for the assessment of insert and keeper lifetimes. Paper presented 41st AIAA/ASME/SAE/ASEE Joint Propulsion Conference & Exhibit. AIAA; Tucson, Arizona, United States of America. <https://doi.org/10.2514/6.2005-4234>
- Mikellides IG, Katz I, Goebel DM, Polk JE, Jameson KK (2006a) Plasma processes inside dispenser hollow cathodes. *Phys Plasmas* 13:063504. <https://doi.org/10.1063/1.2208292>
- Mikellides IG, Katz I, Jameson KK, Goebel DM (2006b) Driving processes in the orifice and near-plume regions of a hollow cathode. Paper presented 42nd AIAA/ASME/SAE/ASEE Joint Propulsion Conference & Exhibit. AIAA; Sacramento, California, United States of America. <https://doi.org/10.2514/6.2006-5151>
- Miller JS, Pullins SH, Levandier DJ, Chiu YH (2002) Xenon charge exchange cross sections for electrostatic thruster models. *J Appl Phys* 91(3):984-991. <https://doi.org/10.1063/1.1426246>
- Polk J, Grubisic A, Taheri N, Goebel DM, Downey R, Hornbeck S (2005) Emitter temperature distributions in the NSTAR discharge hollow cathode. Paper presented 41st AIAA/ASME/SAE/ASEE Joint Propulsion Conference & Exhibit. AIAA; Tucson, Arizona, United States of America. [accessed Mar 20 2020]. <https://www.researchgate.net/publication/254417656>

Sun M, Zhang T, Wu X (2015) [Flow field simulation of 20 cm diameter ion thruster discharge chamber]. *China Optical Journal Network* 27(5):054003. Chinese. <https://doi.org/10.3788/HPLPB20152705.54003>

Sun M, Zhang T, Long J (2017) [Research on plasma characteristics of hollow cathode emitter in a 30-cm ion thruster]. *Propulsion Technology* 38(12):2872-2880. Chinese. <https://doi.org/10.13675/j.cnki.tjjs.2017.12.029>

Sun M, Wang L, Yang J, Wen X, Huang Y, Wang M (2018a) Study of the key factors affecting the triple grid lifetime of the LIPS-300 ion thruster. *Plasma Sci Technol* 20:045504. <https://doi.org/10.1088/2058-6272/aaa66a>

Sun M, Zhang T, Wen X, Guo W, Song J (2018b) Plasma characteristics in the discharge region of a 20A emission current hollow cathode. *Plasma Sci Technol* 20(2):025503. <https://doi.org/10.1088/2058-6272/aa8edb>

Sun M, Zheng Y, Geng H (2020) Grid gap variation of ion thruster during startup in orbit. *IEEE Trans Plasma Sci* 48(2):455-461. <https://doi.org/10.1109/TPS.2020.2965798>

Wirz R, Katz I (2005) Plasma processes of DC ion thruster discharge chambers. Paper presented 41st AIAA/ASME/SAE/ASEE Joint Propulsion Conference & Exhibit. AIAA; Tucson, Arizona, United States of America.